AIAA Guidance, Navigation, and Control Conference
2 - 5 August 2010, Toronto, Ontario Canada

AIAA 2010-8401

Investigation of Energy Management during Approach - Evaluating the Total Energy-Based Perspective Flight-Path Display

M.C.L. van den Hoven,* P.M.A. de Jong,† C. Borst,‡ M. Mulder,§

M.M. van Paassen¶

Delft University of Technology, P.O. Box 5058, 2600 GB Delft, The Netherlands

This paper covers an analysis of the energy management task during the approach phase as well as the design of an experiment supporting this analysis. The energy management task is analyzed using the concept of energy rate demand, which expresses the amount of total energy to be lost in comparison to the minimal energy rate the aircraft can attain at the current speed and configuration. Energy rate demand is explicitly defined by the altitude and speed profile and indicates the demand put on the aircraft by the approach trajectory. A number of approach trajectories are analyzed including a conventional approach, a Continuous Descent Approach (CDA) and a new, experimental, Constant Energy Rate Demand Approach (CERDA). An experiment has been carried out using a total energy-based perspective flight-path display. The results are used to assess the benefits of adding energy information to a tunnel-in-the-sky display and to gain more insight into the energy management task by comparing the different types of energy management as well as energy rate demand with workload and performance. The hypothesis that adding energy information to a baseline tunnel-in-the-sky display will increase the pilot's energy awareness is supported, however, the hypothesis that the workload would decrease with the energy display has been rejected. No relation could be found between energy rate demand, workload, and performance, rejecting the hypothesis that the performance would decrease and the workload increase with increasing energy rate demand.

I. Introduction

The future Air Traffic Management (ATM) system will most likely consist of collaboratively determined 4D business trajectories[1] to cope with the increase in air traffic, delays, as well as a higher demand for safety and reduction in environmental impact.[1] Predecessors of these 4D trajectories are noise abatement procedures, such as Continuous Descent Operations (CDO), which are becoming more common and require high precision flight in order to be effective.[2,3] For these procedures, following a prescribed altitude and speed profile is part of the energy management task and is particularly important during approach.

An approach can be described as a controlled loss of total energy level, which is determined by the altitude and speed profile as commanded by the approach trajectory. A majority of accidents take place during approach and landing[4] and many of them involve incorrect management of the aircraft energy level resulting in either an excess or deficit of total energy.[5] The main factor in these accidents is often found to be an inability to assess or manage the aircraft energy level during approach. Therefore, the approach phase is the part of flight where energy management is most important.

In the past, Amelink[6] has developed a total energy-based perspective flight-path display featuring a tunnel-in-the-sky, Total Energy Angle (TEA) symbol and Total Energy Reference Profile (TERP) to aid the pilot in the energy management task. The original display design has been adapted for this research to eliminate errors and cue mismatches. Amelink has carried out an early experiment to determine how

*MSc. Student, Control and Simulation Division.
†PhD. Student, Control and Simulation Division, AIAA Student Member
‡Postdoctoral Researcher, Aerospace Software and Technologies Institute, AIAA Member
§Professor, Control and Simulation Division, AIAA Senior Member
¶Associate Professor, Control and Simulation Division, AIAA Member

the new display concept could be evaluated. The hypothesis was that the mental workload of the pilot decreases as experience with the display is gained. Since only two pilots were used, the data obtained was not sufficient to test a hypothesis. Therefore, the experiment was performed to find indications of how to continue the work. However, the research did not provide a satisfactory evaluation of the new display format and therefore a new experiment has been carried out to thoroughly evaluate the total energy-based perspective flight-path display.

To analyze the energy management task, the concept of energy rate demand, as introduced by Vormer,[7] is applied to a number of approach trajectories including a conventional approach, CDA and CERDA approach. The energy rate demand is the ratio between the energy rate demanded by the approach trajectory and the maximum energy dissipation the aircraft can attain at the current speed and configuration. It is an indication of how close an aircraft is flying to its operational limits in terms of energy dissipation rates. Therefore, the highest value of energy rate demand indicates the most demanding situation for the aircraft.

The goal of the experiment was to assess the benefits of adding energy information to the tunnel-in-the-sky for increasing the energy awareness and supporting the pilot in the energy management task. Also, the results are used to gain more insight into the energy management task by comparing different types of energy management as well as energy rate demand with workload and performance.

II. Total Energy-Based Perspective Flight-Path Display

To increase the energy awareness and support pilots in the energy management task, Amelink[6] has developed a total energy-based perspective flight-path display, hereafter referred to as the energy display. This display is a Primary Flight Display (PFD) featuring a tunnel-in-the-sky representation enhanced with energy information. The energy relations are visualized to show the structure of the speed and altitude goals, providing the pilot with mechanisms to deal with the manual control task which can be achieved through effective energy management.

The original display design[6] will be discussed in this section. The final display design has been refined in this research to eliminate errors and avoid cue mismatches which were found during an early experiment.[6]

A. Original Display Design

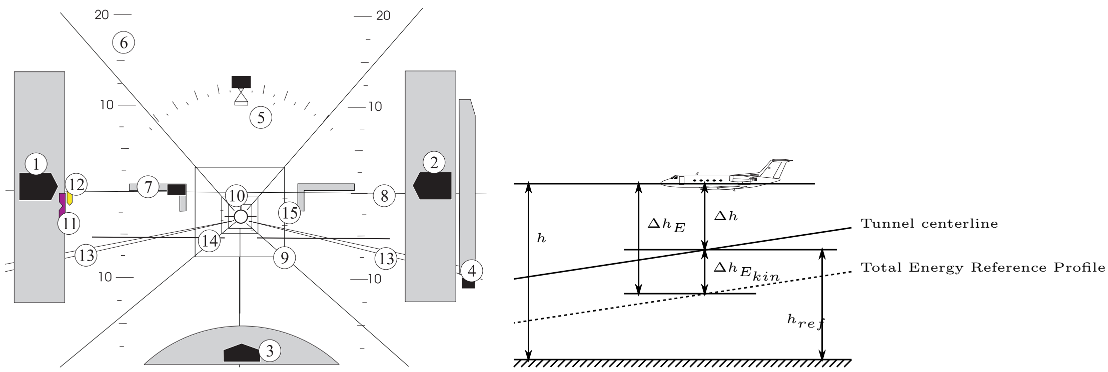

(a) 1) the speed indicator, 2) altitude indicator, 3) compass, 4) vertical speed indicator, 5) bank and slip angle indicator, 6) pitch ladder, 7) aircraft symbol, 8) horizon line, 9) tunnel geometry, 10) FPV symbol, 11) speedbug, 12) speed trend vector, 13) TERP, 14) TEA symbol and 15) speed marks

(b) Definition of the Total Energy Reference Profile (TERP)

Figure 1. The Total Energy-Based Perspective Flight-Path Display[6]

The original display design[6] is depicted in Fig. 1(a). The energy management information presented in the right form is hypothesized to increase the pilot's energy awareness and should allow for more effective energy control strategies. The information is fully integrated in the PFD which is based on a tunnel-in-the-sky display which already determines the form of the display for a great deal.[8] The energy management information is compatible with the tunnel-in-the-sky and display clutter is avoided, especially in the center of the display.

The form of the display reveals the relations between kinetic, potential and total energy in relation to the speed and altitude goals through cues that allow for direct perception. The tunnel trajectory with the Flight Path Vector (FPV) symbol already reveals the potential energy level and rate, however it lacks information about the kinetic and total energy.

The definition of the Total Energy Angle (TEA) and Total Energy Reference Profile (TERP) symbol will be discussed briefly in Section 1 and 2 followed by a description of the energy cues provided by the display in Section 3.

1. *Total Energy Angle (TEA)*

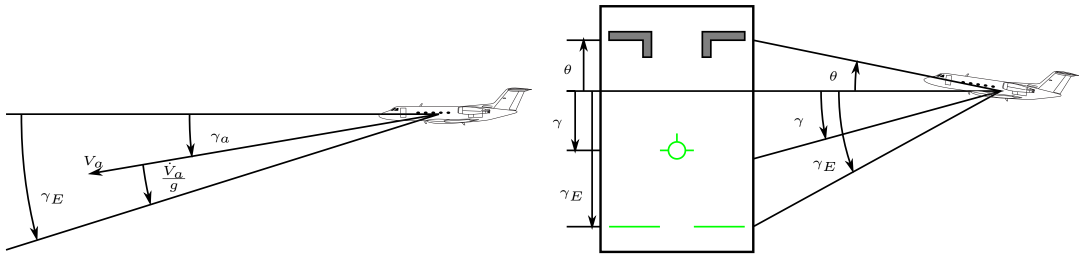

(a) Definition of the Total Energy Angle (TEA) (b) Displayed angles

Figure 2. Angles represented in the Total Energy-Based Perspective Flight-Path Display[6]

The total energy rate is revealed by the TEA symbol, which consists of a green line parallel to the horizon and extents the FPV symbol when aligned. A graphical representation of the energy angle can be found in Fig. 2. The specific non-dimensional total energy rate of the aircraft can be expressed using the TEA γ_E, which is derived from the energy height h_E. The (total) energy height, or specific total energy, is the total altitude that can be reached when instantly exchanging all kinetic energy for potential energy. It is expressed by dividing the total energy E_{tot} by the aircraft weight W. The time derivative of the energy height gives the specific non-dimensional total energy rate $\dot{E}_{sn}$, which defines the TEA, as follows:[6,9]

$$\dot{E}_{sn} = \frac{T - D}{W} = \gamma_a + \frac{\dot{V}_a}{g} = \gamma_E \tag{1}$$

With thrust force T, drag force D, aircraft weight W, aerodynamic flight path angle γ_a, True Airspeed (TAS) V_a and gravitational acceleration g. Throughout this research, zero wind conditions are assumed, meaning the that the TAS V_a is equal to the ground speed V_g at all times. The energy levels are therefore defined in a ground reference frame.

It is assumed that elevator control does not significantly influence drag and therefore, on the short term, the energy angle is controlled only by the throttle. The drag is considered to change only on the long term due to speed changes and changes in aircraft configuration such as the deployment of flaps, landing gear, spoilers and speed brakes. Also, additional induced drag due to vertical maneuvers is neglected.

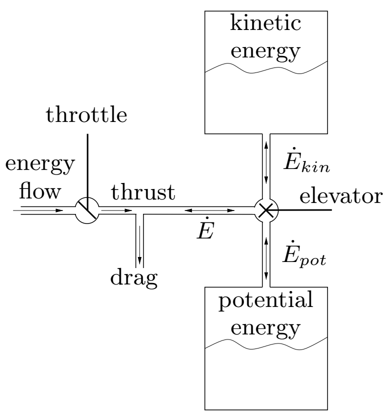

Figure 3. Schematic Representation of the Energy Reservoir Analogy[6]

From Eq. (1) it follows that for a zero (specific non-dimensional) total energy rate ($T = D$), a change in flight path angle γ_a due to an elevator deflection results in potential energy being exchanged into kinetic energy and vice versa, leading to the observation that the elevator controls the distribution of energy whereas the throttle, and on the long term aircraft configuration, controls the total energy rate. This is illustrated in Fig. 3 as a reservoir analogy with two reservoirs, one for kinetic energy and one for potential energy. The flow of energy is controlled by valves which represent the elevator and throttle inputs. As shown in Fig. 3, energy also ‘bleeds’ away from the system by generating drag.

2. Total Energy Reference Profile (TERP)

The sum of the kinetic and potential energy profile yields the Total Energy Profile (TEP), however, knowing the exact total energy level is not important to the pilot and therefore the energy deviation is presented in the display through equivalent heights. The Total Energy Reference Profile (TERP), as defined in Fig. 1(b), can be superimposed as a perspective path on the tunnel-in-the-sky display revealing speed and total energy information.

When the total energy deviation is zero ($\Delta h_E = 0$), the aircraft will be exactly on the TERP and when the kinetic energy deviation is zero ($\Delta h_{E_{kin}} = 0$), the TERP coincides with the tunnel centerline. The speed and altitude goals are satisfied when the aircraft is both on the TERP ánd the tunnel centerline. The TERP is represented as a surface on the sides of the tunnel to avoid clutter in the center of the display resulting in a track-type representation.

3. Energy Cues

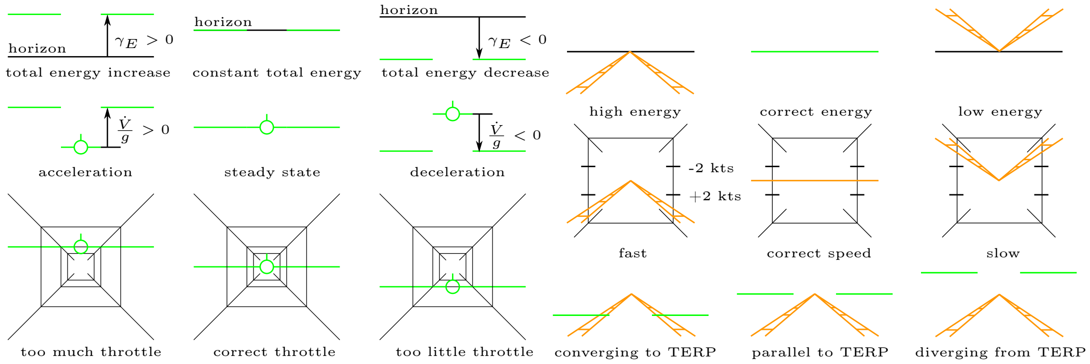

(a) Total Energy Angle (TEA) (b) TERP

Figure 4. Cues Provided by the Energy Display Format[6]

Fig. 4(a) illustrates the cues provided by the TEA symbol. The difference between the FPV symbol and the total energy angle indicates vertical acceleration and it shows the path relative to the tunnel that would be achieved with the current thrust setting in steady state condition. As noted before, the energy angle is controlled through the thrust setting assuming constant drag.

Fig. 4(b) illustrate the cues provided by the TERP. The aircraft’s height above the TERP indicates a surplus of total energy and the vertical distance between the TERP and the tunnel centerline indicates the deviation in commanded ground speed. Speed marks have been added the tunnel to indicate a $\pm$ 2 kts speed margin. Similar to the FPV symbol, the total energy angle symbol indicates the total energy path relative to the TERP. The intersection point indicates the exact intercept location with the TERP.

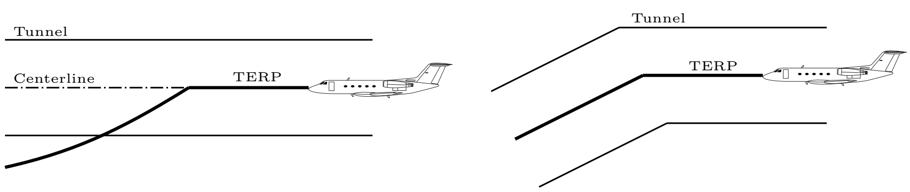

(a) Speed change at constant flight path (b) Flight path change at constant speed

Figure 5. The TERP Provides the Pilot with a Preview of the Commanded Aircraft Energy State[6]

The TERP also provides the pilot with a preview of the commanded aircraft energy state and allows the pilot to anticipate commanded speed and altitude changes as shown in Fig. 5. When the TERP and the tunnel follow the same profile, a flight path change at constant speed is commanded whereas when the TERP moves away from the tunnel, a speed change at constant flight path is commanded. This preview should allow the pilot to better control the aircraft through anticipating what action is required in the near future. This feed-forward control allows for a lower control gain leading to less control activity and better stability.

B. Changes made to Original Display Design

Fig. 12(b) shows a screenshot of the final implemented display design. A few modifications were made to the display based on the findings of an early experiment.[6] From that experiment, it became apparent that pilots confused the flight path cue provided by the FPV symbol and the energy path cue provided by the TEA symbol. They would follow the tunnel with the TEA symbol and the TERP with the FPV symbol instead of the other way around. It is expected that this problem is reduced by giving the TEA symbol and the TERP the same color, in this case yellow. Also, since speed and speed trend information are now transferred through the TERP and TEA, the speed bug and speed trend vector become obsolete and are removed.

In the original implementation, the TERP was defined as a linear interpolation between two energy heights, calculated at the beginning and end of a tunnel segment. However, a quadratic relationship exists between energy height and speed ($h_E = \frac{E_{tot}}{W} = h + \frac{V_a^2}{2g}$) resulting in a parabolic shaped TERP. Although the linear interpolation is acceptable for small decelerations, the error becomes significant for large speed changes, as illustrated in Fig. 6 for an extreme deceleration of 75 Knots Indicated Airspeed (KIAS) per NM. The actual shape of the TERP, however, depends on the required deceleration profile, which is assumed constant throughout each tunnel segment in this case. The linear interpolation therefore provides an incorrect energy level cue to the pilot and has been corrected.

Similar to the TERP definition, the location of the speed marks has been corrected. Also, the appearance of the speed marks is altered and now resembles a flat T-shape alongside the tunnel frames. This gives a clearer upper and lower speed limit that is compatible with the form of the TERP. The speed marks resemble brackets which suggest a restriction in the vertical movement of the TERP.

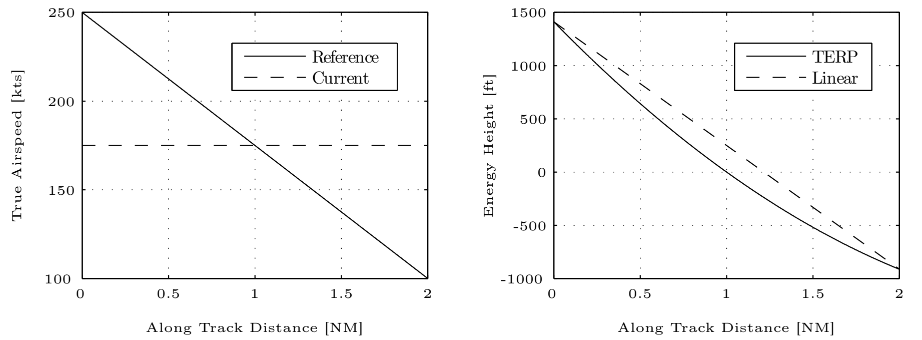

(a) Current and Reference Speed (b) Kinetic Energy Height Deviation $\Delta h_{E_{kin}}$

Figure 6. Comparison between Actual TERP and Linear Interpolation

III. Energy Management during Approach

The energy management task is analyzed using the concept of energy rate demand as introduced by Vormer,[7] which is further elaborated on in this research. The energy rate demand can be derived by applying the aircraft operational constraints to the energy rate efficiency, a ratio which defines how precise the aircraft is flying the prescribed altitude and speed profile in terms of energy rate. Hence, the energy rate demand is a measure for the amount of total energy to be lost in comparison to the maximum energy dissipation the aircraft can attain at the current speed and configuration. Therefore, a higher energy rate demand implies a more demanding energy management task since the aircraft is flying closer to its operating limits. The energy rate demand will be calculated for a number of example approaches, including a conventional, CDA and CERDA approach.

A. Energy Rate Efficiency and Demand

Before moving on to the definition of the energy rate demand, a more general concept will be introduced, the energy rate efficiency, which is defined as the ratio between the current energy rate and the energy rate commanded by the approach trajectory. The energy rate efficiency will be derived from the equations of motion without wind. Throughout this research, zero wind conditions are assumed such that the TAS will equal the ground speed at all times. This also implies that the aerodynamic flight path angle γ_a is always equal to the kinematic flight path angle γ_k, and the angle is defined as downward positive.

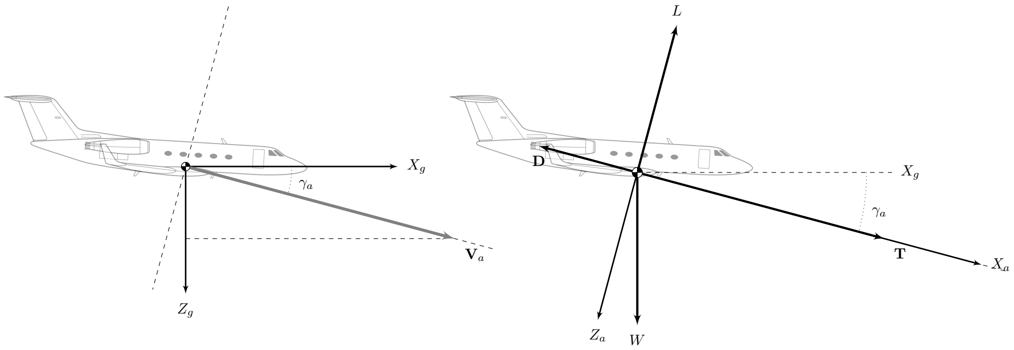

Figure 7. Kinematic (left) and Aerodynamic (right) View of the Aircraft (assuming zero-wind conditions)

Assuming that the aircraft flies a straight approach and changes in aerodynamic flight path are made instantaneously ($\dot{\gamma_a} = 0$), from Fig. 7, the equation of motion in the direction of flight result to:

$$\frac{W}{g}\frac{d}{dt}(V_a) = T - D + W\sin\gamma_a \tag{2}$$

Linearization of Eq. (2) and assuming that the aerodynamic flight path angle is small ($\sin\gamma_a \approx \gamma_a$) yields:

$$\frac{W}{g}\frac{d}{dX_a}(V_a)\frac{dX_a}{dt} = T - D + \frac{W}{V_a}\frac{H}{dt} \tag{3}$$

$$\frac{W}{2g}\frac{d}{dX_a}\left({V_a}^2\right) = T - D + \frac{W}{V_a}\frac{dX_a}{dt}\frac{H}{dX_a} \tag{4}$$

$$\frac{W}{2g}\frac{d}{dX_a}\left({V_a}^2\right) = T - D + \frac{W}{V_a}V_a\frac{H}{dX_a} \tag{5}$$

Rearranging,

$$\frac{W}{2g}\frac{d}{dX_a}\left(V_a^2\right) - W\frac{H}{dX_a} = T - D \tag{6}$$

$$\frac{W}{2g}\frac{d}{dt}\left(V_a^2\right) - W\dot{H} = (T - D)\frac{dX_a}{dt} \tag{7}$$

$$\frac{W}{2g}2V_a\dot{V}_a - W\dot{H} = (T - D)V_a \tag{8}$$

The left hand side of Eq. (8) represents the commanded energy rate, $\dot{E}_{cmd}$, and the right hand side represents the current total energy rate $\dot{E}_{tot}$. Continuing with the commanded energy rate, the speed V_a and flight path angle γ_a are replaced by the commanded variables and using:

$$\dot{H} = V_a\sin\gamma_a \approx V_a\gamma_a \approx V_c\gamma_c \tag{9}$$

Substituting Eq. (9) into the left hand side of Eq. (8) gives:

$$\dot{E}_{cmd} = \frac{W}{g}V_c\dot{V}_c + WV_c\gamma_c \tag{10}$$

The energy rate efficiency $\eta_{\dot{E}}$, can thus be written as:

$$\eta_{\dot{E}} = \frac{\dot{E}_{cmd}}{\dot{E}_{tot}} = \frac{V_cW\left(\gamma_c + \frac{\dot{V}_c}{g}\right)}{V_a(T - D)} \tag{11}$$

The energy rate efficiency is a measure for how close the aircraft is following the energy profile commanded by the approach trajectory. The thrust force is a function of the throttle setting and engine dynamics whereas the drag force is a function of the current TAS and aircraft configuration. An efficiency of 1 indicates that the aircraft is exactly flying the prescribed altitude and speed profile and Eq. (11) reduces to the equation of motion along the flight path, Eq. (8). The goal of the energy management task is therefore to maintain an efficiency of 1, higher will result in a deficit in total energy and lower will result in an excess of total energy.

1. *Energy Rate Demand*

The concept of energy rate efficiency can be applied to the aircraft operational constraints by setting the engine throttle to idle, resulting in minimum thrust force T_{idle}, and therefore the maximum energy dissipation the aircraft can attain at the current speed and configuration. Assuming that the speed of the aircraft equals the commanded speed at all times ($V_a = V_c$), the energy rate demand $\hat{E}$ can be defined as follows:

$$\hat{E} = \frac{W\left(\gamma_c + \frac{\dot{V}_c}{g}\right)}{T_{idle} - D} \tag{12}$$

The energy rate demand is an important parameter in this analysis as it is an indication of how close the aircraft is flying to its operational limits in terms of demanded energy rate. An energy rate demand close to 1 implies that the demanded altitude and speed profile results in a required energy rate which is close to the maximum energy dissipation the aircraft can attain at the current speed and configuration. Therefore, the highest value of energy rate demand indicates the most demanding situation for the aircraft during the approach.

It must be noted that the energy rate demand in this form is only valid when $\gamma_c + \dot{V}_c/g \leq 0$, so typically during approach. When $\gamma_c + \dot{V}_c/g > 0$, the thrust force should be set to maximum to come to a similar definition. The drag force can be controlled through changing the aircraft configuration by deploying flaps, landing gear or speed brakes. A higher drag will increase the energy dissipation rate and therefore the energy rate demand will become smaller. As the energy rate demand increases, this is an indication that a configuration change is needed in order to cope with the required energy rates. This can also be used to define optimal flap and gear schedules for a given approach. Besides that, the energy rate demand can be used to assess the demand of an approach on different types of aircraft, with different thrust and aerodynamic characteristics.

B. Approach Analysis using Energy Rate Demand

The concept of energy rate demand is applied to several sample approaches using a model of the Cessna Citation 500 which is derived from a simulation in DASMAT.[10,11] Two real-life approaches are simulated which are based on the approach onto runway 18R at Amsterdam Airport Schiphol. They include a conventional, stepped descent profile, approach and a CDA, which is typically performed during night-time. The main goal of this analysis is to find out how the energy rate demand relates to different altitude and speed profiles and therefore how it relates to the energy management task. To further assess this relation, a CERDA is defined which will be used in the experiment as explained later on.

1. *Conventional Approach*

The results of this analysis can be found in Fig. 8. The conventional approach is characterized by a step-down descent profile to ensure separation or to decelerate, which is difficult when descending in clean configuration. The energy exchange during level segments is inefficient as the potential energy rate is zero and therefore the kinetic energy rate can only be controlled by the throttle or through changing the aircraft configuration. To optimize the flow of aircraft, high speed is maintained as long as possible and decelerations take place on the level segments and in a 'dirty' configuration at final approach.

Table 1. Flaps and Gear Schedule for the Conventional Approach Analysis

KIAS	Settings
250..171	clean
170..161	flaps 15°, gear down
160..110	flaps 40°, gear down

The flaps and gear schedule used can be found in Table 1. This is a nominal flap schedule for the Cessna Citation 500. When considering the energy rate demand (Fig. 8(e)), it is clear that with this flap schedule the demand stays below 1 at all times indicating that the aircraft is able to fly this approach. To illustrate the effect of configuration changes on the energy rate demand, the clean configuration is shown as well. In clean configuration, the energy rate demand will rise above 1 at the final glideslope indicating that the energy dissipation rate is insufficient and a configuration change is required. This method can also be used to define flap and gear schedules for a certain approach. At some points, the energy rate demand equals zero which is due to a zero flight path angle and zero acceleration meaning that the thrust has to equal the drag to maintain a steady flight condition.

The thrust setting shown in Fig. 8(f) is the setting required to follow the prescribed altitude and speed profile. It can be seen that there are large jumps in the required thrust level due to the level segment of the approach. An energy rate demand close to 1 corresponds to a low thrust level, indicating that at high energy rate demand, the control space for correcting the energy dissipation rate using throttle, diminishes and configuration changes become necessary. The highest energy rate demand occurs during the final stage of the approach where both speed and altitude have to be reduced and therefore energy management is crucial in this phase.

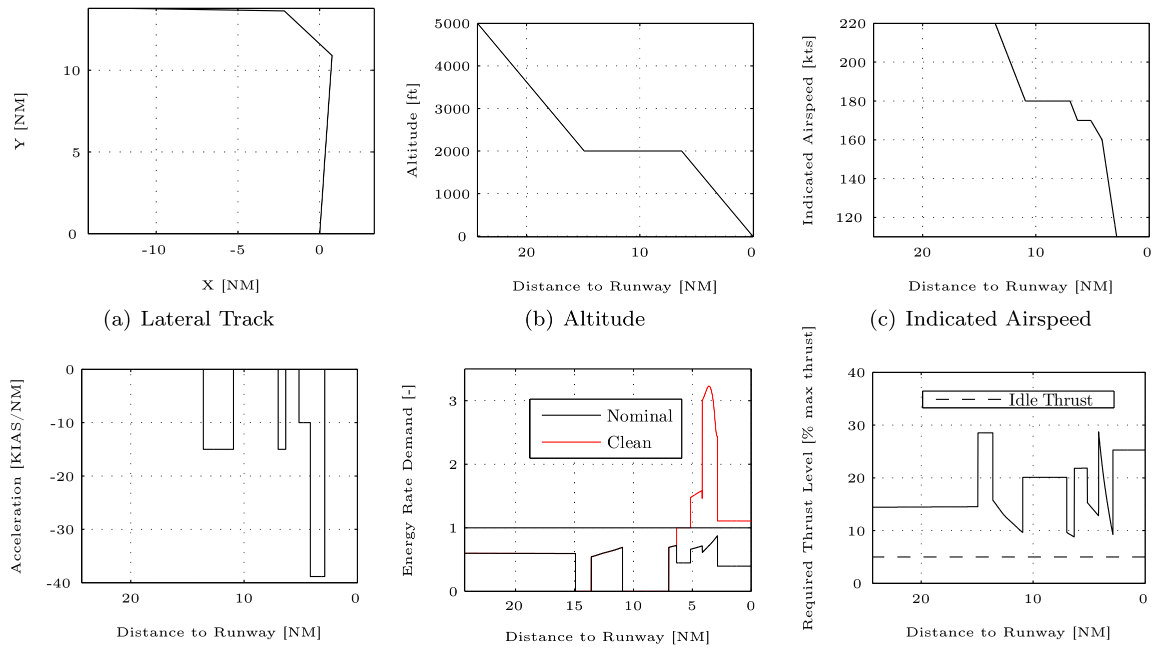

(a) Lateral Track (b) Altitude (c) Indicated Airspeed

(d) Acceleration (e) Energy Rate Demand (f) Thrust Setting

Figure 8. Conventional Approach Analysis based on Schiphol Runway 18R Approach (Cessna Citation 500)

2. Continuous Descent Approach (CDA)

The results of this analysis can be found in Fig. 9. The analysis is based on a typical night transition approach onto runway 18R at Schiphol Airport. Schiphol uses the CDA at night as a noise abatement procedure such that there are no level segments which require additional thrust to maintain speed and altitude leading to increased noise and pollution levels.

The flaps and gear schedule can be found in Table 2 and is based on the flap schedule for the conventional approach. Flaps are deployed earlier on in the approach as decelerating is more difficult when continuously descending. Due to the lack of level segments, the deceleration is more gradual then with the conventional approach. However, the energy rate demand is higher as the aircraft is continuously descending and losing potential energy, which is converted into kinetic energy or bled away through drag. As the flight-path steepens, the energy rate demand increases and flaps and gear deployment becomes necessary. Due to the continuous descent profile, this occurs earlier on in the approach. In comparison to the conventional approach, the average energy rate demand goes up from 0.48 to 0.64 leading to the hypothesis that this is a more demanding approach in terms of energy management. Also, the average required thrust level is lower which satisfies one of the primary goals of a CDA.

Table 2. Flaps and Gear Schedule for the Continuous Descent Approach (CDA) Analysis

KIAS	Settings
250..181	clean
180..171	flaps 15°
170..161	flaps 15°, gear down
160..110	flaps 40°, gear down

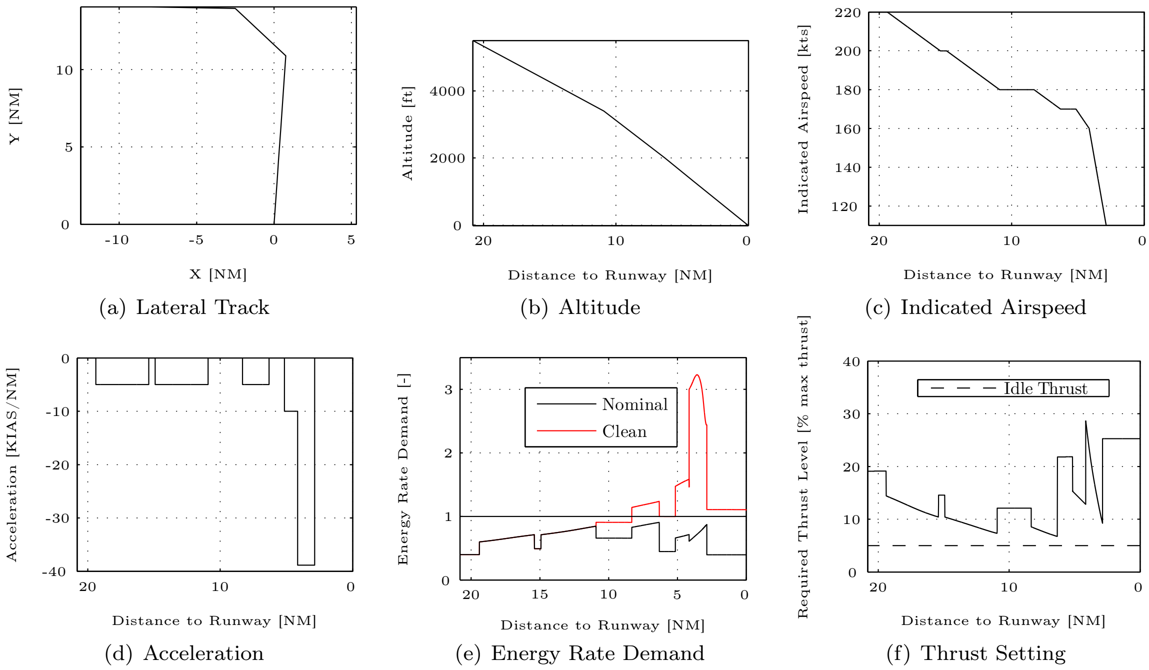

(a) Lateral Track (b) Altitude (c) Indicated Airspeed

(d) Acceleration (e) Energy Rate Demand (f) Thrust Setting

Figure 9. Continuous Descent Approach (CDA) Analysis based on Schiphol Runway 18R Approach (Cessna Citation 500)

3. *Constant Energy Rate Demand Approach (CERDA)*

Following the conventional and CDA approach analysis it can be hypothesized that there is a link between the energy rate demand and the complexity of the altitude and speed profile, or energy management task. In the experiment, an attempt was made to find a connection between energy rate demand and workload, as well as performance. For this reason an approach can be defined with a constant energy rate demand resulting in an altitude and speed profile for which the energy rate demand is fixed. The deviation from this profile is an indication of the tracking performance and it is hypothesized that this performance will decrease with increasing energy rate demand.

Fig. 10 plots an example of the resulting approach with energy rate demands ranging from 0.7 up to 1.0. The altitude profile is based on the CDA approach. With an energy rate demand of 1.0, the approach has to be flown under idle thrust and with correct and timely configuration changes. Lower energy rate demands will still allow room for error such that the pilot can correct deviations from the altitude and speed profile by adjusting thrust setting, flight path or configuration.

The aircraft starts at an initial speed of 250 KIAS and decelerates in such a way that the energy rate demand remains constant towards the approach speed of 110 KIAS at 1,000 ft. The flight path angles can be adjusted to produce different speed profiles for varying energy rate demands. The altitude profile is defined to always end at the stabilization height of 1,000 ft by adjusting the initial altitude to match this condition. A lower energy rate demand implies a more gradual deceleration, and therefore the aircraft will need to start decelerating earlier on in the approach.

The difference in altitude as seen in Fig. 10(b) is caused by the difference in length of the second stretch, again due to the more gradual deceleration at lower energy rate demand. Also, a lower energy rate demand allows aircraft to fly at a higher altitude for a longer time decreasing, for instance, the noise impact. The time window for performing the deceleration to approach speed will decrease with increasing energy rate demand therefore putting more pressure on the pilot indicating that the energy rate demand might be related to the workload and performance.

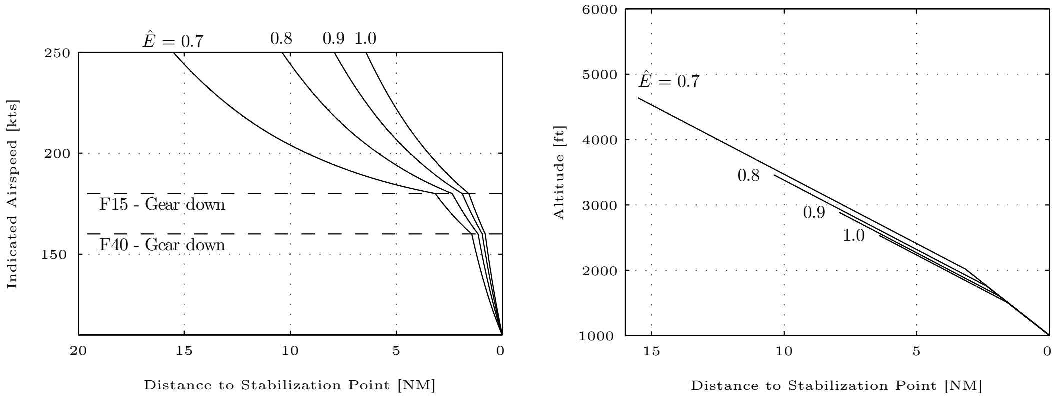

(a) Indicated Airspeed (b) Altitude

Figure 10. Constant Energy Rate Demand Approach (CERDA)

IV. Experiment

A. Goal of the Experiment

The goal of the experiment was to assess the benefits of adding energy information to a tunnel-in-the-sky based PFD for increasing the energy awareness and supporting the pilot in the energy management task. Also, the results have been used to gain more insight into the energy management task by comparing different types of energy management as well as energy rate demand with workload and performance.

B. Method

Subjects and Instructions The experiment involved seven professional pilots with an average age of 46 and 7,100 flying hours. They were instructed to follow the prescribed altitude and speed profile as accurate as possible while maintaining a natural level of control activity. The pilots were given a fixed flap and gear schedule which had to be followed as close as possible. During the training runs, the pilots were encouraged to deviate from the prescribed altitude and speed profile to get acquainted with the different cues provided. Also, pilots were requested to “think aloud” throughout the experiment. They were briefed beforehand about the background, interface design, aircraft model, trajectories and the actual experiment including goal, task, apparatus, procedure etc.

Table 3 gives an overview of the pilot experience. Only two pilots had experience with experimental tunnel-in-the-sky displays and five indicated they had experience with other energy-enhanced displays, mainly featuring a speed trend vector on the speed tape or next to the FPV symbol. Due to a broken log file for the CERDA approaches, one pilot had to be omitted from the analysis of the CERDA scenarios.

Table 3. Overview of the Subject Experience

Subject	Age	Flight hours	Aircraft type	Glass cockpit experience
1	58	4,500	Vast amount of Fokker, Embraer, Boeing and Cessna	yes
2	35	2,600	B747-400, Fokker 70/100, Piper, Cessna, Bee Aircraft	yes
3	65	20,000	B737-800, vast amount of civil and military	yes
4	60	12,700	A310, MD11, G150, CL605, EMB500/505	no
5	31	5,500	A320, B737, single engine piston	yes
6	30	3,250	B737NG, TB200, TB20, C172	yes
7	42	1,050	Cessna 182, 206, Piper Seminole	no

Apparatus The Human-Machine Interaction Laboratory (HMI-Lab) of the Control and Simulation division has been used for the experiment. Fig. 11 shows a picture of the simulator environment which is a fixed-base setup featuring, amongst other things, an 18" LCD monitor, right-handed side-stick, and a pedestal with engine, flap and gear controls. One screen was used displaying the

Figure 11. Human-Machine Interaction Laboratory (HMI-Lab) at Delft University of Technology (DUT)

PFD, while the aircraft could be controlled using the side-stick (3 axes) and throttle. Flap and gear settings can be controlled using the flap and gear levers on the left hand side of the pilot, where also the throttle controls are located. No outside visual nor sound were used in the experiment. The instructor was located in a separate section divided by glass windows from the experiment room.

Independent Variables Two independent, within-subjects variables were defined which are the display mode (DISPLAY) and different trajectories (SCENARIO). DISPLAY had two levels, the baseline and energy display, whereas SCENARIO had six levels, two conventional, stepped descent approaches, two CDA approaches and two CERDA approaches.

Each of the SCENARIO levels require a different type of energy management based on the energy exchange mechanisms. The level segments in the conventional approach require a constant potential energy level where the pilot has to decrease the kinetic energy by decreasing the total energy level. A decrease in speed can be obtained by removing thrust, hence lowering the total energy level, or by deploying flaps/landing gear.

The CDA approach contains segments where it is necessary to maintain speed while descending, meaning that potential energy has to be exchanged for kinetic energy. This makes it easier to maintain speed at lower thrust levels, however it is also more difficult to decelerate, especially in clean configuration.

With the CERDA approaches, the energy rate demand will be kept constant throughout the entire approach. It is chosen to keep the flight path angles fixed, therefore, the speed profile will not be linear, but parabolic as will be explained further on in Section C.

All approaches contain segments where both speed and altitude needs to be lost, hence a full energy management task which requires tight coordination of both the elevator and throttle controls.

The trajectories can be divided into segments where each segment requires a different type of energy management. So the conventional approaches contain many constant potential energy level segments, the CDA approaches many constant kinetic energy level segments and the CERDA approach contains constant energy rate demand segments. Therefore any significant effects found can be related to the type of energy management imposed by the trajectory.

Because the speed profile is based on the Indicated Airspeed (IAS) of the aircraft, a constant reference speed will actually result in a small deceleration when descending, hence a decrease in kinetic energy. This is due to the changing TAS, however, the commanded decelerations are small enough to stay unnoticed by the pilot and a constant kinetic energy level can be assumed.

Dependent Measures A distinction has been made between objective and subjective measurements. The objective measurements include the Root Mean Squared Error (RMSE) of the aircraft vertical position, lateral position, IAS, total energy and total energy rate, which give a good estimate of the magnitude of the error in the tracking task. The vertical and lateral position errors are measured w.r.t. the tunnel centerline. Also, the difference between Actual Time of Arrival (ATA) and Required Time of Arrival (RTA) is used to estimate the 4D performance w.r.t. time requirements. However, 4D operations are not implemented yet and therefore this measure only serves as an indication for future work.

The second objective measure is the control activity. To measure the variability or dispersion of the control inputs, hence the activity, the Standard Deviation (STD) of the control input rates of the elevator, aileron, rudder and throttle is used. By using the rate of control input, any influence of required trim positions is eliminated. This is an indication of pilot workload, more activity means the pilot is working harder to carry out the task.

The subjective measurements include the pilot workload, which will be measured using a NASA Task Load indeX (TLX) rating sheet after each run.[12] The TLX is a multi-dimensional rating procedure that provides an overall workload score based on a weighted average of ratings on six subscales being mental, physical and temporal demands, own performance, effort and frustration.

To measure the pilot's energy awareness for both display modes, an energy awareness questionnaire was given at the end of the experiment. The pilot was asked to rate different tasks (following TERP, tunnel etc.) on a five-point Likert scale for both displays.[13] Following the energy awareness questionnaire, pilots were given a questionnaire with questions about flying experience, simulation realism and general questions about preferences, overall impression, training and any further comments.

Table 4 gives an overview of the dependent measures used in the experiment.

Table 4. Overview of the Dependent Measures

Symbol	Unit	Description
Performance measures		
h_{rmse}	[m]	Root Mean Squared Error (RMSE) of the vertical position
y_{rmse}	[m]	RMSE of the lateral position
$V_{IAS_{rmse}}$	[kts]	RMSE of the IAS
E_{rmse}	[J]	RMSE of the total energy
$\dot{E}_{rmse}$	[J/s]	RMSE of the total energy rate
δRTA	[s]	Difference between ATA and RTA
Control activity measures		
$\sigma_{\dot{\delta}_e}$	[rad/s]	Standard Deviation (STD) of the elevator input rate
$\sigma_{\dot{\delta}_a}$	[rad/s]	STD of the aileron input rate
$\sigma_{\dot{\delta}_r}$	[rad/s]	STD of the rudder input rate
$\sigma_{\dot{\delta}_t}$	[δ/s]	STD of the throttle deflection rate
Workload measure		
WL_{TLX}	[-]	NASA TLX score

Display Description Two display modes were used in the experiment, these are shown in Fig. 12. The baseline display is a tunnel-in-the-sky display which provides a vertical and lateral reference, however, it provides no speed reference. To give the pilots information about the absolute reference speed, next to the speed indicator, a speed bug and speed goal frames were added. The speed bug indicates the speed goal for the current segment and the speed goal frames indicate the location at which this speed has to be obtained. In addition to the speed bug, the target speed, distance to the next speed frame and the next speed goal are shown. This gave the pilot an indication about the required deceleration and speed without showing energy-related information.

With the energy display, the energy state is shown directly through the TERP and the TEA symbol. Therefore, the speed bug and speed goal frame have been removed since the reference speed information is contained in the TERP. The speed marks indicate the ± 2 KIAS speed margin, which also corresponds to the height of the speed bug in the baseline display.

To give the pilot information about the aircraft engine setting and configuration, an engine Revolutions Per Minute (RPM) meter and flaps and gear indicator were added to both displays, respectively. This covers all the state information needed to perform the energy management task. It is chosen to integrate these with the PFD to avoid the need for a navigation display which would only distract the pilot away from the screen. The flap and gear schedule is shown next to the speed tape for both displays.

A tunnel size of 80 m was used with a tunnel frame separation of 0.1 NM. The choice for the tunnel size is based on research done by Mulder and Mulder[14] which states that there exists a trade-off between performance and control activity. A smaller tunnel size leads to higher performance, however, at the cost of an increase in control activity, hence pilot workload. Since it was expected that the energy display would impose a considerable mental demand, it was chosen to define a tunnel minimizing the workload while still leading to an acceptable performance level. The frame separation was chosen to give the pilots another familiar reference for the distance along the tunnel, especially in connection to the distance from the next speed goal frame.

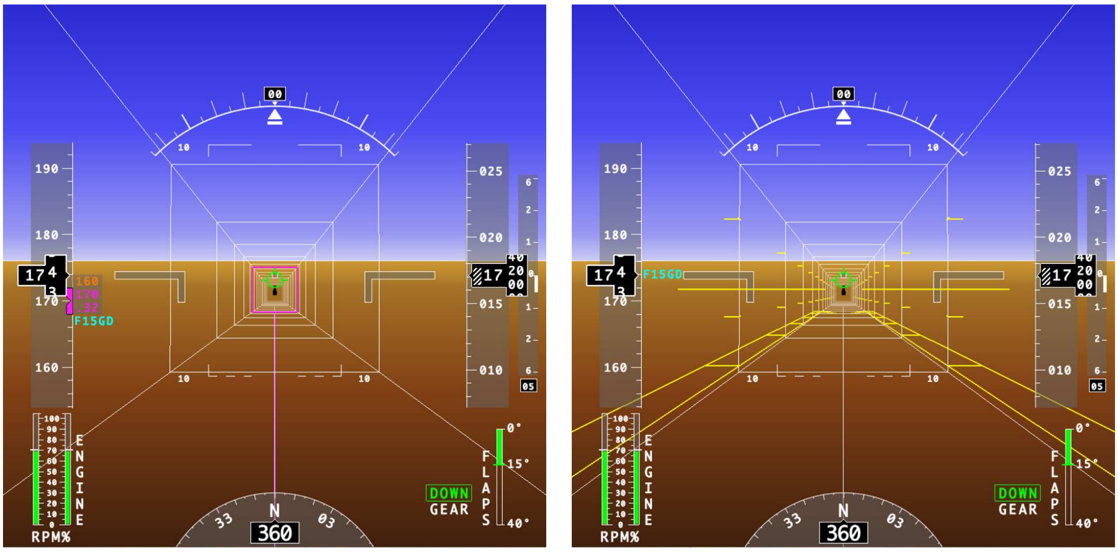

(a) Baseline Tunnel-in-the-sky Display with speed bug and speed goal frames (purple) (b) Total Energy-Based Perspective Flight-Path Display with total energy angle, TERP and speed marks (yellow)

Figure 12. Displayed Modes used in the Experiment

Experiment Design In total there were six scenarios and two display modes. Scenarios 1 and 2 were the conventional, stepped descent approaches, 3 and 4 the CDA approaches, 5 and 6 the CERDA approaches. The conventional and CDA scenarios were mirrored by alternating the direction of turns to avoid recognition and boredom. The two display modes are the baseline display, mode A, and the energy display, mode B. All scenarios and display modes were mixed using a random balanced Latin square design as shown in Table 5.

The experiment started with a training block of at least six runs to make sure the pilot was fully acquainted with the display modes and the different types of scenarios. Basic performance measures were logged to track the pilot's improvements over the training runs. Following the training block, two blocks of six runs were carried out. In total 7 x 6 x 2 = 84 samples were collected.

Table 5. Overview of the Measurement Scenarios

		Block 1						Block 2					
	Run	1	2	3	4	5	6	1	2	3	4	5	6
Subject	1	2B	6B	6A	3B	4B	4A	2A	1B	5A	3A	1A	5B
	2	6B	3B	2B	4A	6A	1B	4B	3A	2A	5B	5A	1A
	3	3B	4A	6B	1B	2B	3A	6A	5B	4B	1A	2A	5A
	4	4A	1B	3B	3A	6B	5B	2B	1A	6A	5A	4B	2A
	5	1B	3A	4A	5B	3B	1A	6B	5A	2B	2A	6A	4B
	6	3A	5B	1B	1A	4A	5A	3B	2A	6B	4B	2B	6A
	7	5B	1A	3A	5A	1B	2A	4A	4B	3B	6A	6B	2B

Procedure First, the pilots were briefed on the experiment and introduced to the different display modes and the HMI-Lab. After that, the training started for at least six runs. This way, the pilot should have seen all type of scenarios and display modes. The pilot was free to request more training on a specific scenario or display until he and the instructor were satisfied with the tracking performance. The briefing and training phase lasted around two hours.

Then, the measurement phase started with two blocks of runs which lasted around one hour each. After each run the pilot was asked to rate his workload using TLX. Between each block, a coffee or lunch break was introduced to avoid boredom and losing focus. At the end of the experiment, the pilot was asked to fill out the energy awareness questionnaire followed by the final questionnaire. Including breaks, the experiment lasted around five hours.

C. Description of the Experiment Simulation

Trajectories The trajectories were based on the conventional, CDA and CERDA approaches. The conventional and CDA approaches consisted of two different routes with straight segments alternated by turns. The turns were defined with a bank angle of 15° followed by a recovery segment. In the conventional approach scenarios, the turns and recovery segments are level to avoid energy exchange, however for the CDA they are descending to maintain the continuous descent characteristics. The speed during turns and recovery is always kept constant to minimize the required energy management. Fig. 13 gives an overview of the altitude and speed profiles that have been used in the experiment.

The CERDA approaches were all defined straight-in with an energy rate demand of 0.1 or 0.8. The first approach consists of a long level segment followed by the final glideslope with a very gradual deceleration profile resulting in a low energy rate demand of 0.1. The other approach consists of a very steep descent profile with glideslopes up to 4.5° resulting in a high energy rate demand of 0.8. The conventional and CDA approaches have a Root Mean Squared (RMS) energy rate demand of 0.54 and 0.61, respectively.

The parabolic shape of the speed profile in the CERDA scenarios is due to a non-linear deceleration profile caused by a combination of constant energy rate demand and constant flight path angle. Also, the drag characteristics of the aircraft change with changing TAS and configuration. The deceleration can be calculated by rewriting Eq. (12):

$$\dot{V}_c = \left[\frac{(T_{idle} - D)\,\hat{E}}{W} - \gamma_c \right] g \tag{13}$$

Where the idle thrust T_{idle}, energy rate demand $\hat{E}$, aircraft weight W, commanded flight path angle γ_c and gravitational acceleration g remain constant and the drag force D varies with the TAS and aircraft configuration. From Eq. (13), the complete speed profile can be calculated for each segment of the approach.

Aircraft Model and Experiment Conditions The aircraft model used is a six-degree of freedom non-linear model of the Cessna Citation 500.[10] It is trimmed for each trajectory's initial altitude and IAS in clean configuration. An International Standard Atmosphere (ISA) condition was used with zero-wind conditions to reduce the number of independent variables and to simplify the calculation of the TERP.

Simulation Software The simulation ran on DUECA[15] which is a framework for the implementation of (real-time) programs developed at Delft University of Technology (DUT) and programmed in C++. DUECA is a middleware environment for the implementation of processes characterized by a data-flow architecture on a distributed computing network, in this case the HMI-Lab. The lab has a number of computers, or nodes, which are connected to the different components, e.g. the controls, displays, outside visuals, sound system etc. These nodes communicate with each other through DUECA.

D. Hypotheses

It was expected that adding energy information to the baseline tunnel-in-the-sky display will increase the pilot's energy awareness and tracking performance while lowering the workload. Pilots, in a previous experiment,[6] indicated an increase in energy awareness and the same result was expected here. Also, it was hypothesized that the benefits of the energy display become more apparent when the energy management task would be more difficult. This difficulty can be expressed through the different types of energy management as well as through the energy rate demand. The hypothesis was that the performance will decrease and the workload will increase with increasing energy rate demand, because the pilot will need to operate the aircraft close to its operational limits.

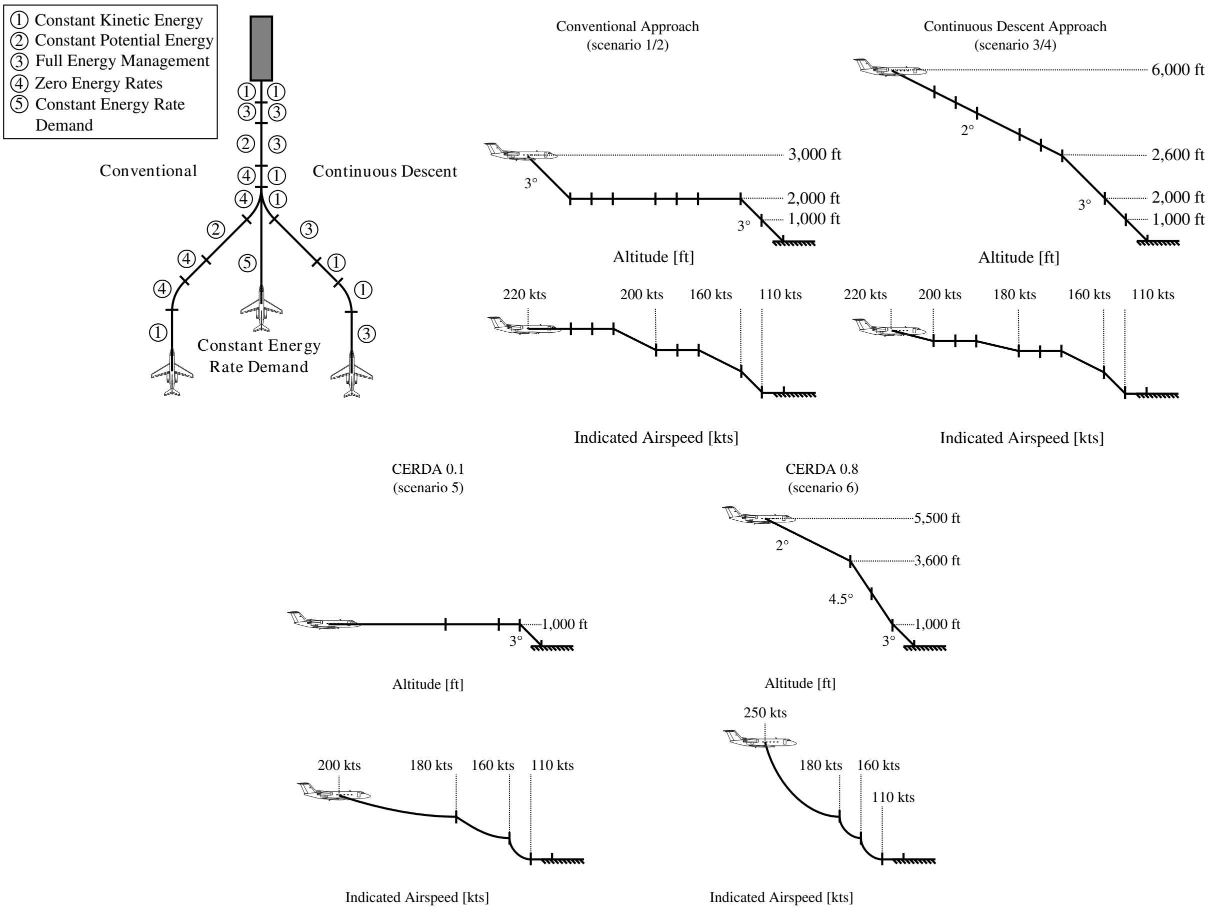

Figure 13. Schematic Representation of the Scenarios used in the Experiment

V. Experiment Results

The analysis is divided into two parts, first the conventional and CDA scenarios are analyzed, followed by the CERDA scenarios. It is chosen to analyze these separately as the first resemble real-life situations, whereas the CERDA approaches are experimental. Also, the speed profiles differ significantly to be able to maintain a constant energy rate demand on the CERDA approaches. As opposed to the conventional and CDA scenarios, the deceleration profile does not follow fixed steps, making it a different tracking task, as can also be seen in Fig. 13.

All the data were divided in segments after which only the straight segments are used in the analysis. This is done to rule out the influence of turns which were only used to avoid recognition and boredom.

A. Conventional and CDA Scenarios

This analysis covers the first four scenarios, 1 and 2 are the conventional approaches, 3 and 4 the CDA approaches. The two sets of approaches were mirrored and therefore the altitude and speed profiles are equal for scenario 1-2 and 3-4.

A check for a significant difference between the mirrored scenarios has been carried out. If there is no difference, scenario 1-2 and 3-4 can be analyzed as repetitions, as if the pilot has flown the exact same scenario twice. Due to the assumption that the mirrored scenarios are repeated, the number of samples double and significant effects should become more clear.

To determine which type of statistical test can be applied to the measures a normality check has been carried out using the Shapiro-Wilk Test.[16] To check for a significant difference between the mirrored scenarios, a Paired-Samples T-test[17] was applied to the normally distributed measures. The Wilcoxon Signed-Rank Test[18] was used for the non-normally distributed measures.

It follows that for the lateral offset y_{rmse} a significant difference between scenario 1 and 2 was found (Wilcoxon, $z = -2.028$, $p = 0.043$), as well as for scenario 3 and 4 (t-test, $t_6 = 3.165$, $p = 0.019$). The lateral offset has therefore been analyzed for all four scenarios instead of combining the mirrored ones. For all other measures, no significant differences were found and the mirrored scenarios could be combined. Fig. 14 shows the box and error bar plots, depending on the sample distribution, showing the 95% confidence intervals.

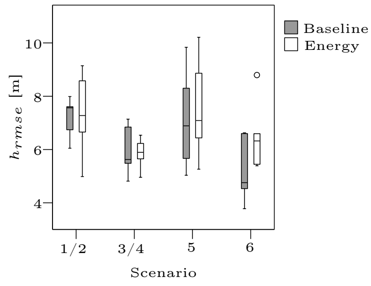

(a) Vertical offset

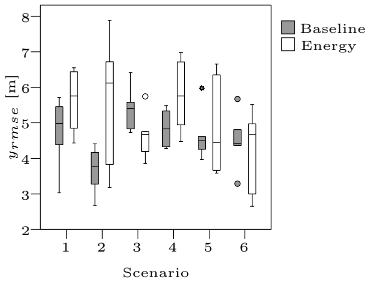

(b) Lateral offset

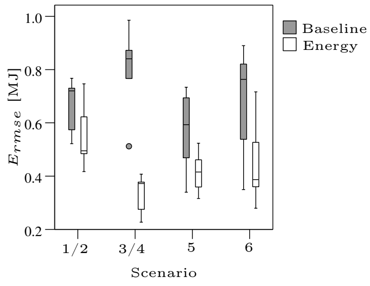

(c) Total energy offset

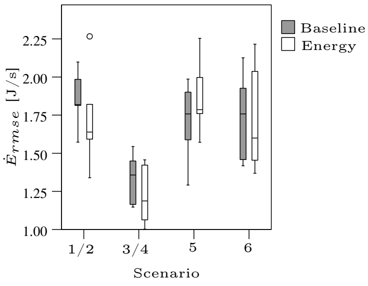

(d) Total energy rate offset

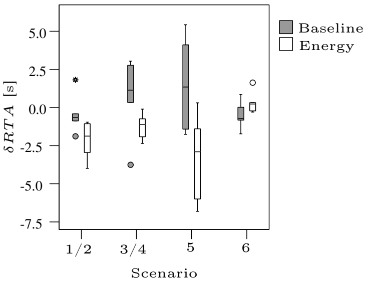

(e) RTA offset

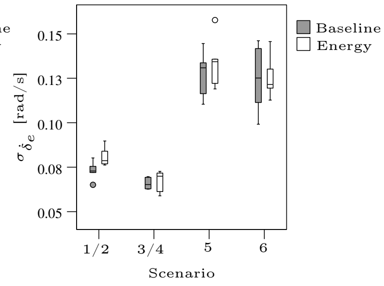

(f) Elevator activity

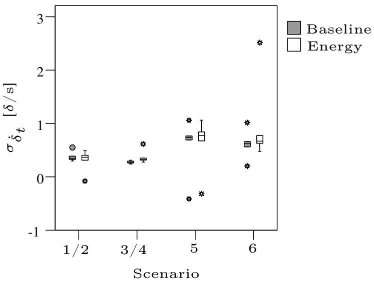

(g) Throttle activity

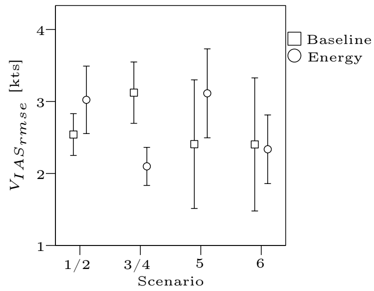

(h) Speed offset

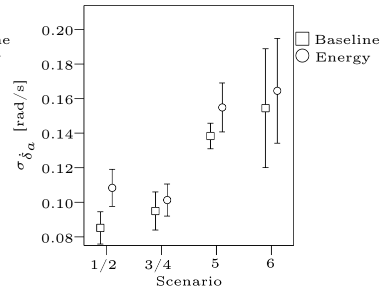

(i) Aileron activity

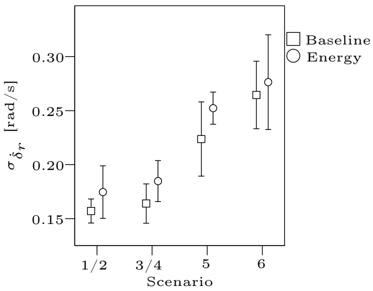

(j) Rudder activity

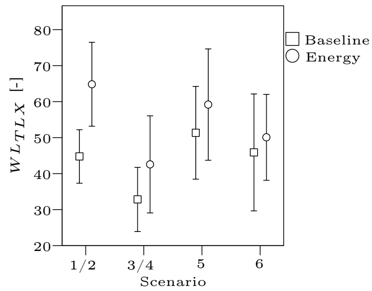

(k) Workload

Figure 14. Box and Error Bar Plots

The lateral offset is analyzed first using the Wilcoxon Test for the non-normally distributed measures and an Analysis of Variance (ANOVA) for the normally distributed measures. Only the straight segments were taken into account and therefore, the speed and altitude profile did not influence the lateral performance and both tests showed no significant effects of display mode nor scenario.

For the remaining measures, the mirrored scenarios could be combined, doubling the number of samples for scenario 1-2 and 3-4. A normality check using the Shapiro-Wilk Test showed that, afterwards, more measures were normally distributed allowing for more powerful statistical tests to be applied to the data.

Since an ANOVA assumes the sample to be normally distributed, this can not be applied to the non-normally distributed measures. Instead, the Friedman Test is applied, which is a non-parametric alternative to the parametric repeated measures ANOVA.[19] This is applied to the total energy rate offset

$\dot{E}_{rmse}$, RTA difference δRTA and throttle activity $\sigma_{\dot{\delta}_t}$. For all other measures, an ANOVA is used for which the results can be found in Table 6, together with the results of the Friedman Test.

Table 6. Results of the Full-Factorial ANOVA for Combined Scenarios 1-2 and 3-4 (chance level $p \leq 0.05$ represents significant effects)

	h_{rmse}	$V_{IAS_{rmse}}$	E_{rmse}	$\dot{E}_{rmse}{}^a$	δRTA^a	$\sigma_{\dot{\delta}_e}$	$\sigma_{\dot{\delta}_a}$	$\sigma_{\dot{\delta}_r}$	$\sigma_{\dot{\delta}_t}{}^a$	WL_{TLX}
Main effects										
SCENARIO	⋆⋆	·	·	⋆	·	⋆⋆	·	·	·	⋆
DISPLAY	·	∘	⋆⋆	·	·	·	⋆	⋆⋆	·	⋆
Two-way interactions										
SCENARIO X DISPLAY	·	⋆⋆	⋆	·	·	·	⋆⋆	·	·	·

⋆⋆, ⋆ and ∘ represent chance levels of $p \leq 0.01$, $0.01 < p \leq 0.05$ and $0.05 < p \leq 0.10$, respectively
[a] Friedman's Two-Way ANOVA by Rank

The decrease in workload on the CDA scenarios (ANOVA, $F_{1,6} = 11.151$, $p = 0.016$) is caused by the speed profile. Due to the lower deceleration levels, as opposed to the conventional scenarios, pilots had more time to interpret the information and carry out the speed changes leading to an increase of their vertical and energy rate performance (h_{rmse}: ANOVA, $F_{1,6} = 18.489$, $p = 0.005$; $\dot{E}_{rmse}$: Friedman, $p = 0.043$). This also resulted in a lower elevator control activity (ANOVA, $F_{1,6} = 18.382$, $p = 0.005$).

Due to the lower workload found for the CDA scenarios, pilots had more time to interpret the information given by the TERP and TEA symbol, such that the speed and total energy level performance increased for the energy display ($V_{IAS_{rmse}}$: ANOVA, $F_{1,6} = 21.703$, $p = 0.003$; E_{rmse}: ANOVA, $F_{1,6} = 13.424$, $p = 0.011$). The same result, however, could not be found for the conventional scenarios. Also, the aileron control activity decreased with the energy display on the CDA scenarios (ANOVA, $F_{1,6} = 20.678$, $p = 0.004$). It followed that the performance with the energy display depends on the mental demand required by the energy management task. A higher mental demand leads to a decrease in mental capacity available to the pilot, which is needed to interpret the energy display format. However, pilots indicated in the questionnaires that the mental demand for the energy display would probably decrease with more training, leading to different results.

Overall, a significant total energy level performance increase (ANOVA, $F_{1,6} = 29.069$, $p = 0.002$) was found for the energy display. Also, the aileron and rudder control activity increased ($\sigma_{\dot{\delta}_a}$: ANOVA, $F_{1,6} = 12.063$, $p = 0.013$; $\sigma_{\dot{\delta}_r}$: ANOVA, $F_{1,6} = 18.998$, $p = 0.005$) leading to a higher workload (ANOVA, $F_{1,6} = 6.884$, $p = 0.039$). Though not significant, an increase in elevator and throttle control activity was found as well. This supports the statement that the mental demand is higher for the energy display as opposed to the baseline display.

B. CERDA Scenarios

Again for the CERDA scenarios, the measures are first checked for normality using the Shapiro-Wilk Test. Based on these results, Friedman's Two-Way ANOVA by Rank was applied to the non-normally distributed measures and a full-factorial ANOVA was carried out for the normally distributed measures. Both of the tests showed no significant effects so the Wilcoxon Signed-Rank Test was applied, which did show significant results.

Here as well, the lower deceleration levels on scenario 5 lead to a significant total energy level performance increase for the energy display (Wilcoxon, $z = -1.992$, $p = 0.046$). Besides that, no significant differences between scenario 5 and 6 could be found. Overall, the control activity levels were higher for the CERDA scenarios as opposed to the conventional and CDA scenarios, but this was not reflected in the workload. Since the aircraft was flown close to the operating limits on the CERDA scenarios, pilots probably had more difficulty controlling the aircraft, leading to the higher control activities.

The large spread in the throttle activity for scenario 5 was caused by the inaccuracy of the throttle quadrant. For this scenario, it was required to apply only minor throttle changes which were difficult to carry out with the current throttle quadrant. When the pilots noticed that a throttle change did not have any effect they tried to compensate with large throttle deflections. This might have influenced the results for scenario 5 and therefore care was taken when interpreting the results.

C. Questionnaires

1. *Energy Awareness Questionnaire*

A statistical analysis was carried out on the results of the energy awareness questionnaire. The energy awareness questionnaire consisted of a number of questions where the pilot is asked to rate a certain task on a five-point Likert scale.[13] These tasks were all related to energy management, for instance maintaining speed and altitude, estimating energy levels etc. The rating was done for the baseline and energy display, so a comparison can be made between both display modes in terms of energy awareness. The responses to the questions are ordinal data, therefore, the Wilcoxon Signed-Rank Test was used.

Due to the common mistake made by pilots following the TERP with the FPV symbol instead of the tunnel lead to the response that the altitude estimation was better with the baseline display (Wilcoxon, $z = -2.333$, $p = 0.020$). Also, the combination of the TEA and TERP helped the pilots with setting the correct throttle level and therefore the effect of a throttle input on the total energy level was more apparent with the energy display (Wilcoxon, $z = -1.992$, $p = 0.046$).

2. *Final Questionnaire*

No statistical analysis was carried out for the final questionnaire since no comparisons are made in the questions. However, a summary will be given of the pilot responses to the different questions.

The realism of the simulation was rated average to realistic for the altitude and speed profile as well as the flap and gear schedule. The simulator environment was rated unrealistic to average, mainly because of the poor control characteristics of the control stick and a dead zone in the throttle quadrant. Five out of seven pilots rated the aircraft dynamics as realistic, two rated it as average to very unrealistic.

All pilots understood, or rated neutral, the tunnel-in-the-sky format, FPV symbol, speed bug and speed goal frames relation, speed bug and the flap and gear schedule. Most pilots understood the relation between the TEA symbol and the throttle input, TEA symbol and TERP and the TERP position relative to the tunnel centerline. One pilot did not understand all previous relations and probably failed to master the energy display format. He also did not comprehend the speed marks and the relation between the TERP and total energy level, which the others did. All pilots indicated they understood, or rated neutral, how to detect oncoming speed changes and carry them out for both display modes.

Six pilots indicated they found the linking of display components through coloring useful, one rated it neutral. On the question which display mode the pilots preferred, four answered the baseline display, two the energy display and one said neutral.

D. Comments and Open Questions

Due to the tunnel-in-the-sky representation, pilots did not use the speed tape and attitude indicators anymore leading to a low absolute Situational Awareness (SA) which some found disturbing. Also, with the energy information added, pilots did not even look at the speed indicator anymore because the speed information was already contained in the TERP.

Pilots found it difficult to assess whether the TERP commanded a speed change or flight path change due to the track-type representation resembling a path. This lead to pilots sometimes steering towards the TERP when actually a speed change was commanded, which could magnify the error even further. They, however, found it easier to detect the required deceleration with the energy display due to the continuous indication of energy level.

The lack of absolute reference speed indication in the energy display was found disturbing, however, the lack of speed trend information in the baseline display as well. Some pilots indicated that the energy level was easier to determine using the speed indication than the TERP because of the unfamiliar format. But it was also noticed that this might be solved with more training. The responses indicated that the speed bug and speed goal frames lead to better speed awareness and provides checkpoints to control the trajectory.

Almost all pilots found the immediate response of the TEA symbol to throttle inputs and flap and gear changes very useful as it shows the influence on energy level in a direct sense. There were some comments on the simulator environment, especially on the stick control laws and a dead zone in the throttle quadrant. The side-stick did not provide any force feedback and therefore felt over-sensitive and unrealistic. The dead zone in the throttle quadrant was due to calibration problems and inaccuracy of the throttle controls due to wear.

The flap and gear schedule indication was often missed by the pilots as their attention was drawn towards the TERP with the energy display. Some suggested to make the indication blink or add sound signals to warn the pilot about upcoming flap and gear changes.

E. Experiment Observations

During the experiment, it became clear that pilots sometimes followed the TERP instead of the tunnel, especially when switching between display modes. This was due to the track-type representation of the TERP confusing the pilots.

One pilot mentioned that the commanded task can be better performed by the autopilot with the energy display as a monitoring tool. As expected, turns were difficult to handle because the TERP and the TEA symbol are always defined in the vertical direction, parallel to the horizon.[6] When flying at a banked angle, it becomes difficult to assess the energy level because the energy information is presented at a different angle than the aircraft's attitude. Also, following the tunnel in turns was often a challenge for the pilots, because they found it difficult to find the correct placement of the FPV symbol.

Pilots found it difficult to assess whether or not they were on the tunnel centerline. It was also noticed that, during training, some pilots consistently flew at the edge of the tunnel because they found it easier to follow just one of the splay lines. Also, because with the energy display small changes in energy level were reflected instantaneously, pilots seemed to be steering with a larger control gain which lead to the higher workload, as mentioned before.

F. Discussion

The hypothesis that adding energy information to the baseline tunnel-in-the-sky display will increase the pilot's energy awareness is supported. The energy display provides mechanisms to better maintain a total energy level and shows the direct response of throttle inputs and configuration changes on the total energy level. This lead to a performance increase, but only in the scenarios with a low mental demand, which were the CDA scenarios and the CERDA approach with an energy rate demand of 0.1. Therefore, the hypothesis that the workload would decrease with the energy display has been rejected.

Overall, it was found that the mental demand is higher for the energy display as opposed to the baseline display, but with enough mental capacity available to the pilot, higher performance levels can be obtained. It is expected that through better training, the mental demand for the energy display can be lowered, such that less mental capacity is required which will lead to higher performance levels on more demanding tasks as well.

It appears that the performance with the energy display is related to the speed profile of the approach trajectory. Using the energy display, performance was high and workload low during the CDA approach and the CERDA approach ($\hat{E} = 0.1$) which both have a gradual deceleration profile. While flying these approaches, the pilots had more time to interpret the information provided by the displays and the benefits of the energy display became apparent. No relation could be found between energy rate demand, workload, and performance, rejecting the hypothesis that the performance would decrease and the workload increase with increasing energy rate demand. It was found, however, that the amount of deceleration demanded by the trajectory is a measure for the mental demand, due to the limited amount of time available to the pilot for carrying out speed changes.

No significant effects could be found for the 4D performance. Both display modes allow for high precision flight, usually within a $\pm$ 5 KIAS speed margin resulting in a minor impact on RTA deviation. During the experiment, pilots noticed that such high precision is never required in actual flight. However, this remark is based on present day operations, whereas this research focuses on future, high-precision flight.[1]

From the questionnaires, it became clear that a combination of both displays is preferred, as the baseline display gives an absolute reference of the required speed, whereas the energy display gives a clear reference for the throttle position and a continuous indication of the required energy level. Combining both displays will give a complete representation of the aircraft energy state and provides cues to correct deviations from this state.

VI. Conclusions and Recommendations

In this research, the original display design[6] for a total energy-based perspective flight-path display has been improved based on the findings of an early experiment.[6] From that experiment, it became apparent that pilots confused the flight path cue provided by the FPV symbol and the energy path cue provided by the TEA symbol. They would follow the tunnel with the TEA symbol and the TERP with the FPV symbol instead of the other way around. It was expected that this problem could be solved by matching the colors of the TEA and TERP, the problem, however, persisted during the new experiment. Pilots found it difficult to assess whether the TERP commanded a flight path or speed change, due to the track-type representation.

The energy management task has been analyzed using the concept of energy rate demand.[7] The energy rate demand can be derived by applying the aircraft operational constraints to the energy rate efficiency, a ratio which defines how precise the aircraft is flying the prescribed altitude and speed profile in terms of energy rates. Hence, the energy rate demand is a measure for the amount of total energy to be lost in comparison to the maximum energy dissipation the aircraft can attain at the current speed and configuration. Therefore, a higher energy rate demand implies a more demanding energy management task since the aircraft is flying closer to its operating limits. It was hypothesized that the energy rate demand is related to the workload and performance, such that the performance would decrease and the workload increase with increasing energy rate demand.

To complete the investigation on energy management during approach, an experiment has been carried out using the total energy-based perspective flight-path display. The experiment provides a thorough evaluation of the display, which has not been done before, and was set up as a comparison between a baseline tunnel-in-the-sky display, and the energy display. The goal of the experiment was to assess the benefits of adding energy information to a tunnel-in-the-sky based PFD for increasing the energy awareness and supporting the pilot in the energy management task. Also, the results have been used to gain more insight into the energy management task by comparing different types of energy management as well as energy rate demand with workload and performance.

The hypothesis that adding energy information to the baseline tunnel-in-the-sky display will increase the pilot's energy awareness is supported, however, the hypothesis that the workload would decrease with the energy display has been rejected. Overall, it was found that the mental demand is higher for the energy display as opposed to the baseline display, but with enough mental capacity available to the pilot, higher performance levels can be obtained. It is expected that through better training, the mental demand for the energy display can be lowered which will lead to better results.

It appears that the performance with the energy display is related to the speed profile of the approach trajectory, however, no relation could be found between energy rate demand, workload, and performance, rejecting the hypothesis that the performance would decrease and the workload increase with increasing energy rate demand. From the questionnaires, it became clear that a combination of both displays is preferred, as the baseline display gives an absolute reference of the required speed, whereas the energy display gives a clear reference for the throttle position and a continuous indication of the required energy level.

It is recommended to investigate the influence of changing wind conditions as they have a significant effect on the aircraft's energy state which will be directly shown using the energy display. For future experiments, it is further recommended to use a more realistic simulator environment, with improved stick control laws and throttle quadrant, as this was a major complaint of the pilots. Also, more training is required to further reduce the mental demand for the energy display, improving the performance.

References

[1] SESAR Consortium, "SESAR Master Plan," April 2008, SESAR Definition Phase - Deliverable 5.

[2] Erkelens, L. J. J., "Advanced Noise Abatement Procedures for Approach and Departure," *AIAA Guidance, Navigation, and Control Conference and Exhibit, Montery, California*, August 2002.

[3] Ren, L., Clarke, J.-P. B., and Ho, N. T., "Achieving Low Approach Noise without Sacrificing Capacity," *Digital Avionics Systems Conference, 2003. DASC '03. The 22nd*, Vol. 1, October 2003, pp. 1.E.3–1.1–9.

[4] Boeing Commercial Airplanes - Aviation Safety, "Statistical Summary of Commercial Jet Airplane Accidents - Worldwide Operations 1959-2008," Internet (`http://www.boeing.com/news/techissues`), July 2009.

[5] Airbus, "Airbus Flight Operations Briefing Notes: Approach Techniques - Aircraft Energy Management during Approach," Internet (`http://www.airbus.com/index.php?id=781`), October 2005.

[6] Amelink, M. H. J., Mulder, M., van Paassen, M. M., and Flach, J., "Theoretical Foundations for a Total Energy-Based Perspective Flight-Path Display," *The International Journal of Aviation Psychology*, Vol. 15, No. 3, July 2005, pp. 205–231.

[7] Vormer, F. J., *Theoretical and Operational Aspects of Optimal Airport Arrival Trajectories*, Ph.D. thesis, Delft University of Technology, 2005.

[8] Mulder, M., *Cybernetics of tunnel-in-the-sky displays*, Ph.D. thesis, Delft University of Technology, 1999.

[9] Borst, C., *Ecological Approach to Pilot Terrain Awareness*, Ph.D. thesis, Delft University of Technology, 2009.

[10] Van der Linden, C., *Delft University Aircraft Simulation Model and Analysis Tool*, Delft University Press, 1998.

[11] Van Paassen, M. M., Gernaey, J., in 't Veld, A. C., and Mulder, M., "Using Ecological Interface Design for Energy Management during Idle-Thrust Approaches," *Proceedings of the 14th International Symposium on Aviation Psychology, Dayton, Ohio*, 2007, pp. 727–782.

[12] Hart, S. G. and Staveland, L. E., "Development of NASA-TLX (Task Load Index): Results of Empirical and Theoretical Research," *Human Mental Workload*, 1988, pp. 139–183.

[13] Likert, R., "A Technique for the Measurement of Attitudes," *Archives of Psychology*, Vol. 22, No. 140, 1932, pp. 55.

[14] Mulder, M. and Mulder, J. A., "Cybernetic Analysis of Perspective Flight-Path Display Dimensions," *Journal of Guidance, Control, and Dynamics*, Vol. 28, No. 3, May-June 2005, pp. 398–411.

[15]Van Paassen, M. M., Stroosma, O., and Delatour, J., "DUECA - Data-Driven Activation in Distributed Real-Time Computation," *Proceedings of the AIAA Modeling and Simulation Technologies Conference and Exhibit, Denver (CO)*, 2000.

[16]Shapiro, S. S. and Wilk, M. B., "An Analysis of Variance Test for Normality (Complete Samples)," *Biometrika*, Vol. 52, No. 3/4, December 1965, pp. 591–611.

[17]Field, A., *Discovering Statistics using SPSS*, SAGE Publications Ltd, London, 3rd ed., 2009.

[18]Wilcoxon, F., "Individual Comparisons by Ranking Methods," *Biometrics Bulletin*, Vol. 1, No. 6, December 1945, pp. 80–83.

[19]Friedman, M., "A Correction: The Use of Ranks to Avoid the Assumption of Normality Implicit in the Analysis of Variance," *Journal of the American Statistical Association*, Vol. 34, No. 205, March 1939, pp. 109.